MICHIGAN STATE UNIVERSITY

CYCLOTRON LABORATORY

# TWO-PROTON CORRELATION FUNCTIONS FOR EQUILIBRIUM AND NON-EQUILIBRIUM EMISSION

W.G. GONG, C.K. GELBKE, N. CARLIN, R.T. de SOUZA, Y.D. KIM, W.G. LYNCH, T. MURAKAMI, G. POGGI, D. SANDERSON, M.B. TSANG, H.M. XU, D.E. FIELDS, K. KWIATKOWSKI, R. PLANETA, V.E. VIOLA, Jr., S.J. YENNELLO, and S. PRATT

MARCH 1990

MSUCL-718

MSUCL-718
March, 1990

# "Two-proton correlation functions for equilibrium and non-equilibrium emission"

W.G. Gong, C.K. Gelbke, N. Carlinf B.T. de Sousa, Y.D. Kim, W.G. Lynch, T. Murakami,* G. Poggi,tt D. Sanderson, M.B. Tsang, and H.M. Xu
National Superconducting Cyclotron Laboratory
and Department of Physics and Astronomy,
Michigan State University, East Lansing, MI 48824, USA

D.E. Fields, K. Kwiatkowski, R. Planeta, V.E. Viola, Jr., and S.J. Yennello
Indiana University Cyclotron Facility
and Departments of Chemistry and Physics
Indiana University, Bloomington, IN 47405, USA

S. Pratt
Department of Physics, University of Wisconsin, Madison, WI 53706, USA

Abstract: Two-proton correlation functions are compared for equilibrium and non-equilibrium emission processes investigated, respectively, in "reverse kinematics" for the reactions $^{129}Xe+^{27}Al$ and $^{129}Xe+^{122}Sn$ at E/A=31 MeV and in "forward kinematics" for the reaction $^{14}N+^{197}Au$ at E/A=75 MeV. Observed differences in the shapes of the correlation functions are understood in terms of the different time scales for equilibrium and preequilibrium emission. Transverse and longitudinal correlation functions are very similar.

---

† Present address: Instituto de Física, Universidade de São Paulo, C. Postal 20516, CEP 01498, São Paulo, Brazil

* Present address: Department of Physics, Kyoto University, Kyoto 606, Japan

tt Permanent address: Dipartimento di Fisica dell' Università and INFN, Largo Enrico Fermi 2, 50125 Firenee, Italy

Two protons, emitted at small relative momenta from an excited nuclear system, carry information about the space-time characteristics of the emitting source [1-10]. The shape of the two-proton correlation function reflects the interplay of the short-range attractive nuclear interaction, the Pauli exclusion principle, and the long range repulsive Coulomb interaction between the two emitted protons. The short range nuclear interaction is dominated by the attractive singlet S-wave nuclear interaction which leads to a pronounced maximum in the two-proton correlation function at relative momentum q≈20 MeV/c, when the average distance upon emission is of the order of 10 fm or less [1]. The long range Coulomb interaction and the Pauli exclusion principle give rise to a minimum at q=0. Some directional information is provided by antisymmetrization effects [1,7,8] which are important when $|\vec{q}\cdot\vec{r}|<h$, where $\vec{q}$ and $\vec{r}$ denote the relative momentum and position vectors upon emission.

The average distance between two coincident protons upon emission depends on the spatial dimension, d, of the emitting system and on the time interval, $\tau$, between the two emission processes; it is of the order of $d+\bar{v}\tau$, where $\bar{v}$ is the average velocity of the emitted protons. For the decay of equilibrated compound nuclei with temperatures below 5 MeV, estimated emission times are larger than several hundred fm/c [11]. As a consequence, the average distance between emitted particles is much larger than the size of the emitting nucleus and the effects of the Coulomb interaction and the Pauli principle should dominate. On the other hand, preequilibrium light particle emission in intermediate energy heavy ion collisions is calculated to proceed on much shorter time scales [12,13] and average particle separations may reflect the spatial dimension of the emitting system rather than the emission rate. Here, the nuclear interaction should be prominent.

In this letter, we report a comparative study of two-proton correlation functions measured for preequilibrium and equilibrium emission processes. When light projectiles impinge on heavy target nuclei, preequilibrium emission is strongly enhanced at small angles, whereas equilibrium emission dominates at backward angles, see e.g. refs. [5,10]. Preequilibrium emission was studied in "forward kinematics" for the reaction $^{14}N+^{197}Au$ at E/A=75 MeV. Equilibrium emission was studied at a lower energy, E/A=31 MeV, in "reverse kinematics" for the reaction $^{129}Xe+^{27}Al$ and for the nearly-symmetric system $^{129}Xe+^{122}Sn$.

The experiments were performed with beams from the K1200 cyclotron from the National Superconducting Cyclotron Laboratory at Michigan State University. We used $^{27}Al$, $^{122}Sn$, and $^{197}Au$ targets with areal densities of 5.6, 5.3, and 15.9 $mg/cm^2$, respectively. Light particles were detected with two $\Delta E$-E detector arrays consisting of 300-400 $\mu m$ thick silicon $\Delta E$-detectors and 10 cm long CsI(Tl) or NaI(Tl) E-detectors. An array consisting of 37 Si-CsI(Tl) telescopes [14] was centered at the polar and azimuthal angles of $\theta=25^\circ$ and $\phi=0^\circ$; each of its detectors had a solid angle of $\Delta\Omega=0.37$ msr and a nearest neighbor spacing of $\Delta\theta=2.6^\circ$. Another array consisting of 13 Si-NaI(Tl) telescopes was centered at $\theta=25^\circ$ and $\phi=90^\circ$; each of its detectors had solid a angle of $\Delta\Omega=0.5$ msr and a nearest neighbor spacing of $\Delta\theta=4.4^\circ$. Coincidence and downscaled singles data were taken simultaneously. Energy calibrations are accurate to better than 2%. Typical detector energy resolutions were of the order of 2% and 1% for protons of 40 MeV and 100 MeV, respectively. All data were corrected for random coincidences.

The two-particle correlation function, R(q), is defined in terms of the coincidence yield, $Y_{12}(\vec{p}_1,\vec{p}_2)$, and the single particle yields, $Y_1(\vec{p}_1)$ and $Y_2(\vec{p}_2)$:

$$\Sigma Y_{12}(\vec{p}_1,\vec{p}_2) = C_{12}[1+R(q)]\Sigma Y_1(\vec{p}_1)Y_2(\vec{p}_2) \ . \qquad (1)$$

Here, $\vec{p}_1$ and $\vec{p}_2$ are the laboratory momenta of particles 1 and 2, and q is the relative momentum of the particle pair. For each experimental gating condition, the sums on both sides of Eq. 1 are extended over all energy and detector combinations corresponding to the given bins of q. The normalization constant, $C_{12}$, is determined by the requirement that R(q)=0 for large relative momenta.

Two-proton correlation functions measured for the $^{14}N+^{197}Au$ reaction are shown in Fig. 1. A strong dependence on the total laboratory momentum, P, of the coincident proton pair is measured, consistent with previous observations [2-6,8]. The solid curves show theoretical correlation functions predicted for sources of Gaussian density, $\rho(r) \propto \exp(-r^2/r_0^2)$, and negligible lifetime, providing an upper limit for the size of the emitting system. For the high total momentum gates, rapid nonequilibrium processes dominate and the neglect of temporal effects may be justifiable [8]. The lowest total momentum gate selects protons of low energy, E≈10-20 MeV, for which contributions from equilibrated target residues may be important. For this gate, the shape of the minimum at q≈0 can only be reproduced by short-lived sources of unphysically large dimensions (dashed curve) or by long-lived evaporative sources discussed below (dotted curve).

Two-proton correlation functions measured for the $^{129}Xe+^{27}Al$ and $^{129}Xe+^{122}Sn$ reactions at E/A=35 MeV are shown in Fig. 2. They exhibit a minimum at q≈0, but no maximum at q≈20 MeV/c. Correlation functions of similar shape were reported for equilibrium emission in the $^{16}O+^{27}Al$ [9] and $^{40}Ar+Ag$ [10] reactions at E/A=8.75 and 44 MeV, respectively. The data shown in Fig. 2 correspond to proton energies slightly above the compound nucleus Coulomb barrier and are expected to be dominated by emission from long-lived equilibrated composite nuclei formed in incomplete fusion reactions [15]. For the $^{129}Xe+^{27}Al$ reaction, the total momentum gate P=660-750 MeV/c selects energies, in the center-of-mass frame of reference, $E_{cm}$≈15-23 MeV; for the $^{129}Xe+^{122}Sn$ reaction, the gates P=540-660 MeV/c and P=660-750 MeV/c select the energies $E_{cm}$≈15-27 MeV and $E_{cm}$≈27-40 MeV, respectively. For total momenta selecting center-of-mass energies below the Coulomb barrier, the minimum in the two-proton correlation function at q≈0 becomes narrower and washes out for the lowest energies (not shown in the figure). We refrain from a discussion of correlation functions for sub-barrier emission, since it requires a thorough understanding of the shape of the exit channel Coulomb barrier and its penetration, as well as other complicating effects, such as sequential decays of primary fragments emitted in particle unbound states [11].

Correlation functions for particle evaporation from long-lived compound nuclei can be calculated by using the Wigner-function formalism of ref. [7]. We have performed such calculations for the simple evaporative model of ref. [11]. In this model, the level density is approximated by that of an ideal Fermi gas at normal nuclear density. The results, averaged over the appropriate momentum bins and folded with the resolution of the experimental apparatus, are shown by the dotted curve in Fig. 1 and the solid, dashed, and

dotted curves in Fig. 2. The parameters used in these calculations (initial mass, $A_i$, charge, $Z_i$, and temperature, $T_i$, of the decaying nucleus) are indicated in the figures. Since emission rates depend mainly on the temperature [11] and less strongly on the mass and charge number of the emitting nucleus, we used the compound nucleus values for $A_i$ and $Z_i$, but treated $T_i$ a free parameter. For complete fusion of $^{129}Xe+^{27}Al$ and $^{129}Xe+^{122}Sn$, temperatures of 8.2 and 10.3 MeV, respectively, are calculated if one assumes the level density of an ideal Fermi gas of normal nuclear matter density; the more common relation, $T^2=(8\ MeV)\times E^*/A$, gives values of 5.8 and 7.3 MeV. However, the equilibrated emitting systems should have somewhat lower temperatures [5,15-17] since some energy is carried away by preequilibrium emission. Good agreement between calculations and the data for the Xe-induced reactions is obtained with initial temperatures of about 5-7 MeV. The calculations are sufficiently sensitive to the initial temperature to rule out significantly higher values. For the $^{14}N+^{197}Au$ reaction, the assumption of emission from an equilibrated nucleus is less justified; the reproduction of the data in the low momentum gate is somewhat worse.

The dependence of the two-particle correlation function on the angle, $\Psi = \cos^{-1}(\vec{P}\cdot\vec{q}/Pq)$, between the relative and total momentum vectors of the two-proton pair can provide clues on the source lifetime and shape [1,7,8]. Qualitatively, emission from a long-lived system will resemble a source elongated in the longitudinal direction [7,8]. Because of the reduced Pauli anti-correlation in this direction, the longitudinal correlation function ($\Psi\approx 0^\circ$ or $180^\circ$) of a long-lived source may be enhanced compared to the transverse correlation function ($\Psi\approx 90^\circ$), unless the average particle separations become so large that sensitivity to antisymmetrization effects is lost. Very similar

longitudinal and transverse correlation functions were measured [8], at $\theta \approx 30^\circ$, for the $^{32}S+Ag$ reaction at E/A=22.3 MeV. These results ruled out long lifetime effects for the emission of preequilibrium light particles. Our data for the $^{14}N+^{197}Au$ reaction are qualitatively consistent with those of ref. [8]. More recently, differences between longitudinal and transverse correlation functions of the order of 20% were reported [10] for back-angle emission in the Ar+Ag reaction at E/A=44 MeV which is dominated by emission from equilibrated residues formed in incomplete fusion reactions. We have evaluated longitudinal and transverse correlation functions for the Xe-induced reactions, by applying cuts of $\Psi_\ell = 0^\circ$-$40^\circ$ or $140^\circ$-$180^\circ$ and $\Psi_t = 60^\circ$-$120^\circ$. In Fig. 3, our data are shown by the open and solid points; calculations with the indicated parameters are shown by the solid and dotted curves. (In order to increase the statistical accuracy, the momentum gates have been made wider than in Fig. 2.) No statistically significant difference between longitudinal and transverse correlation functions is measured. This result is in accordance with the calculations. However, the calculations predict more significant differences between longitudinal and transverse correlations functions at higher total momenta and for narrower momentum gates. Unfortunately, the statistical accuracy of our experiment was insufficient to confirm these predictions.

In summary, we have measured two-proton correlation functions for equilibrium and preequilibrium emission processes. Correlation functions measured for preequilibrium emission exhibit a pronounced maximum at relative momenta $q \approx 20$ MeV/c and a minimum at $q \approx 0$ MeV/c which are, respectively, caused by the attractive singlet S-wave interaction between the two emitted protons and the combined effects of the Coulomb repulsion and the Pauli principle; the time scales are sufficiently short that memory of the size of the emitting system

is retained. Correlation functions observed for evaporative processes do not exhibit a maximum at q≈20 MeV/c, but only the minimum at q≈0 MeV/c; large emission time intervals lead to large separations between emitted particles and a loss of memory of the size of the emitting nucleus. Two-proton correlation functions measured in kinematic regions dominated by equilibrium emission could be quantitatively reproduced by statistical model calculations based on the Weisskopf formula. For the present system, no significant differences between longitudinal and transverse correlation functions were found, in agreement with statistical model calculations which predict them to be below the sensitivity of our measurement. Our observations support a picture of the collision in which the smaller impacting nucleus generates a forward spray of energetic particles in a relatively short time scale, leaving a heated heavy reaction residue which emits particles over a longer period of time while cooling evaporatively.

This work is based upon work supported by the National Science Foundation under Grant numbers PHY-86-11210 and PHY-89-13813 and the Department of Energy under grant number DE.FG02-88ER.40404.A000. WGL acknowledges the receipt of U.S. Presidential Young Investigator Award and NC acknowledges partial support by the FAPESP, Brazil.

References

1. S.E. Koonin, Phys. Lett. 70B (1977) 43.

2. W.G. Lynch, C.B. Chitwood, M.B. Tsang, D.J. Fields, D.R. Klesch, C.K. Gelbke, G.R. Young, T.C. Awes, R.L. Ferguson, F.E. Obenshain, F. Plasil, R.L. Robinson and A.D. Panagiotou, Phys. Rev. Lett. 51 (1983) 1850.

3. Z. Chen, C.K. Gelbke, J. Pochodzalla, C.B. Chitwood, D.J. Fields, W.G. Lynch and M.B. Tsang, Phys. Lett. B186 (1987) 280.

4. Z. Chen, C.K. Gelbke, W.G. Gong, Y.D. Kim, W.G. Lynch, M.R. Maier, J. Pochodzalla, M.B. Tsang, F. Saint-Laurent, D. Ardouin, H. Delagrange, H. Doubre, J. Kasagi, A. Kyanowski, A. Péghaire, J. Péter, E. Rosato, G. Bizard, F. Lefèbvres, B. Tamain, J. Québert, and Y.P. Viyogi, Phys. Rev. C36 (1987) 2297.

5. J. Pochodzalla, C.K. Gelbke, W.G. Lynch, M. Maier, D. Ardouin, H. Delagrange, H. Doubre, C. Grégoire, A. Kyanowski, W. Mittig, A. Péghaire, J. Péter, F. Saint-Laurent, B. Zwieglinski, G. Bizard, F. Lefèbvres, B. Tamain, and J. Québert, Y.P. Viyogi, W.A. Friedman, and D.H. Boal, Phys. Rev. C35 (1987) 1695.

6. J. Pochodzalla, C.B. Chitwood, D.J. Fields, C.K. Gelbke, W.G. Lynch, M.B. Tsang, D.H. Boal, and J.C. Shillcock, Phys. Lett. B174 (1986) 36.

7. S. Pratt and M.B. Tsang, Phys. Rev. C36 (1987) 2390.

8. T.C. Awes, R.L. Ferguson, F.E. Obenshain, F. Plasil, G.R. Young, S. Pratt, Z. Chen, C.K. Gelbke, W.G. Lynch, J. Pochodzalla, and H.M. Xu, Phys. Rev. Lett. 61 (1988) 2665.

9. P.A. DeYoung, M.S. Gordon, Xiu qin Lu, R.L. McGrath, J.M. Alexander, D.M. de Castro Rizzo, and L.C. Vaz, Phys. Rev. C39 (1989) 128.

10. D. Ardouin, F. Guilbault, C. Lebrun, D. Ardouin, S. Pratt, P. Lautridou, R. Boisgard, J. Québert, and A. Péghaire, University of Nantes, Internal Report LPN-89-02.

11. W.A. Friedman and W.G. Lynch, Phys. Rev. C28 (1983) 16.

12. J. Aichelin and G. Bertsch, Phys. Rev. C31 (1985) 1730.

13. W. Cassing, Z. Phys. A329 (1988) 471.

14. W.G. Gong, Y.D. Kim, G. Poggi, Z. Chen, C.K. Gelbke, W.G. Lynch, M.R. Maier, T. Murakami, M.B. Tsang, H.M. Xu, and K. Kwiatkowski, Nucl. Instr. and Meth. A268 (1988) 190.

15. R. Wada, D. Fabris, K. Hagel, G. Nebbia, Y. Lou, M. Gonin, J.B. Natowitz, R. Billerey, B. Cheynis, A. Demeyer, D. Drain, D. Guinet, C. Pastor, L. Vagneron, K. Zaid, J. Alarja, A. Giorni, D. Heuer, C. Morand, B. Viano, C. Mazur, C. Ngô, S. Leray, R. Lucas, M. Ribrag, and E. Tomasi, Phys. Rev. C39 (1989) 497.

16. D.X. Jiang, H. Doubre, J. Galin, D. Guerreau, E. Piasecki, J. Pouthas, A. Sokolov, B. Cramer, G. Ingold, U. Jahnke, E. Schwinn, J.L. Charvet, F. Frehaut, B. Lott, C. Magnago, M. Morjean, Y. Patin, Y. Pranal, J.L. Uzureau, B. Gatty, and D. Jacquet, Nucl. Phys. A503 (1989) 560.

17. H.M. Xu, W.G. Lynch, C.K. Gelbke, M.B. Tsang, D.J. Fields, M.R. Maier, D.J. Morrissey, T.K. Nayak, J. Pochodzalla, D.G. Sarantites, L.G. Sobotka, M.L. Halbert, and D.C. Hensley, Phys. Rev. C40 (1989) 186.

Figure Captions:

Fig. 1: Two-proton correlation functions measured for the $^{14}N+^{197}Au$ reaction at E/A=75 MeV for the indicated gates on the total momentum, P, of the two-proton pair. The solid and dashed curves show predictions for Gaussian sources of negligible lifetime and the dotted curve shows calculations for an evaporative source with parameters indicated on the figure.

Fig. 2: Two-proton correlation functions measured for the $^{129}Xe+^{27}Al$ (part a) and $^{129}Xe+^{122}Sn$ (parts b,c) reactions at E/A=31 MeV for the indicated gates on the total momentum, P, of the two-proton pair. The curves represent calculations for evaporative sources with parameters indicated on the figure.

Fig. 3: Longitudinal and transverse two-proton correlation functions measured for the $^{129}Xe+^{27}Al$ (top) and $^{129}Xe+^{122}Sn$ (bottom) reactions at E/A=31 MeV for the indicated gates on the total momentum, P, of the two-proton pair. The curves represent calculations for evaporative sources with parameters indicated on the figure.

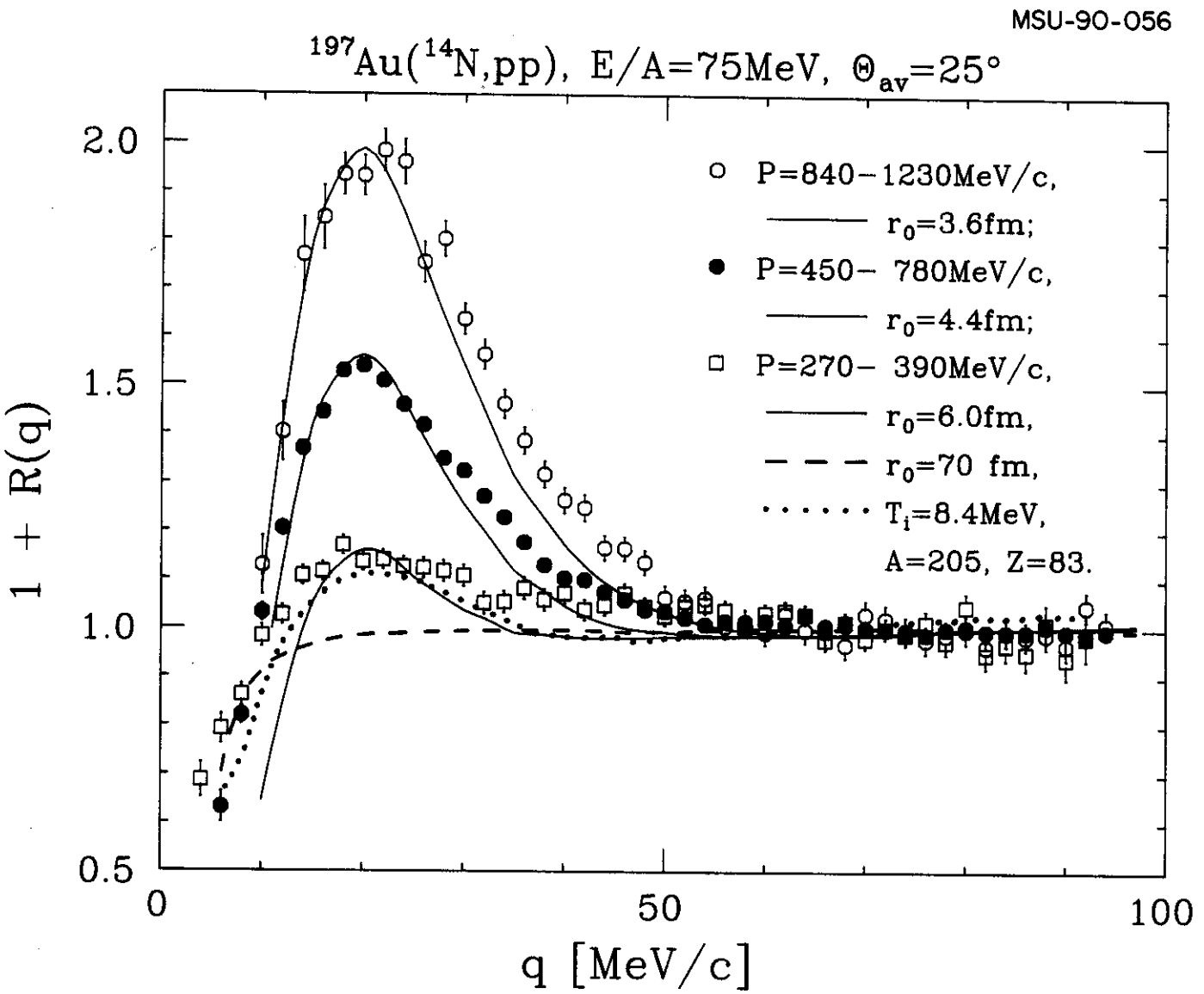
MSU-90-056
$^{197}$Au($^{14}$N,pp), E/A=75MeV, $\Theta_{av}$=25°
P=840−1230MeV/c,
$r_0$=3.6fm;
P=450− 780MeV/c,
$r_0$=4.4fm;
P=270− 390MeV/c,
$r_0$=6.0fm,
$r_0$=70 fm,
$T_i$=8.4MeV,
A=205, Z=83.
1 + R(q)
2.0
1.5
1.0
0.5
0
50
100
q [MeV/c]

Fig. 1

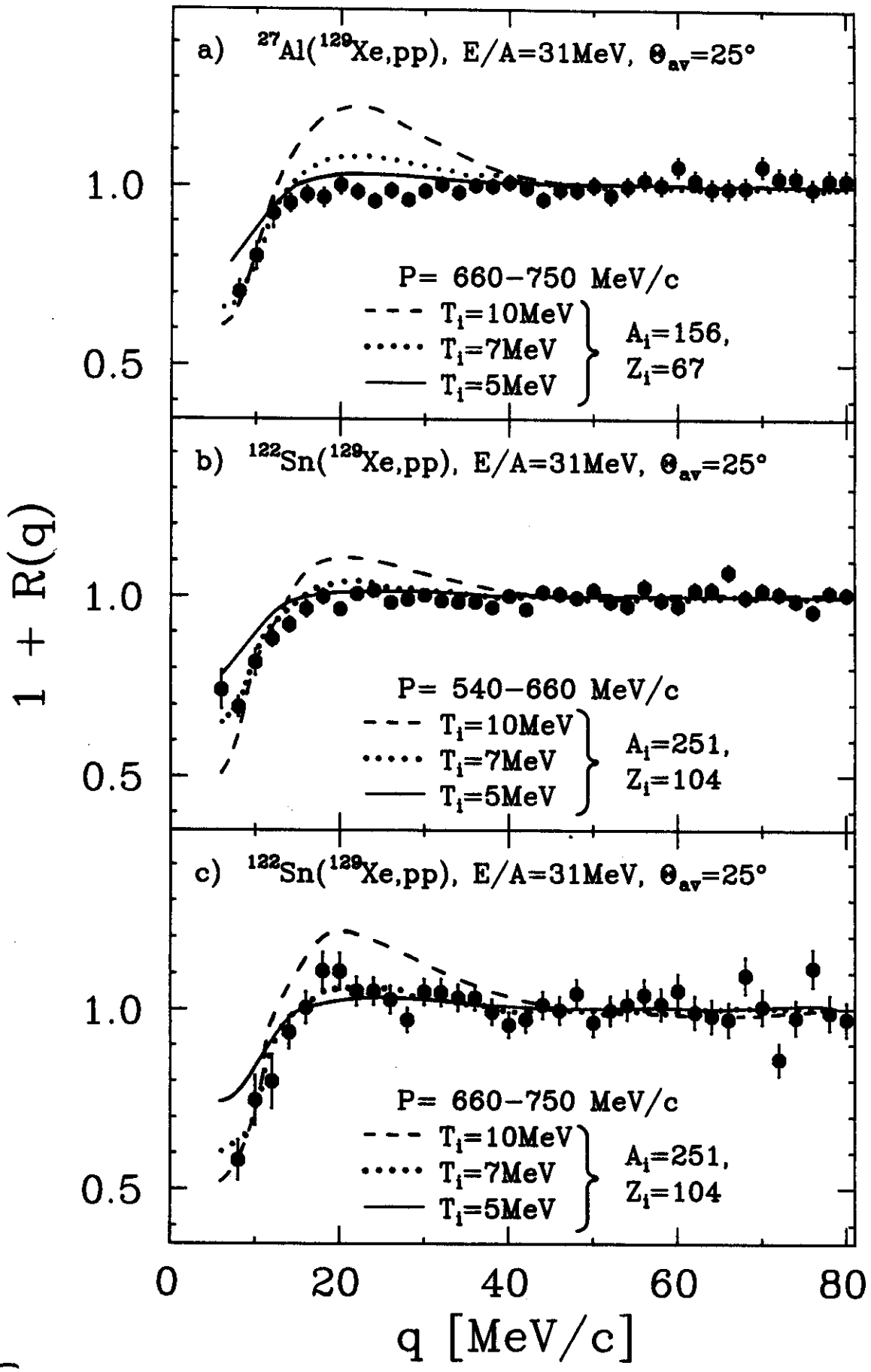
a) $^{27}$Al($^{129}$Xe,pp), E/A=31MeV, $\theta_{av}$=25°
P= 660−750 MeV/c
$T_i$=10MeV
$T_i$=7MeV
$T_i$=5MeV
$A_i$=156,
$Z_i$=67
b) $^{122}$Sn($^{129}$Xe,pp), E/A=31MeV, $\theta_{av}$=25°
P= 540−660 MeV/c
$T_i$=10MeV
$T_i$=7MeV
$T_i$=5MeV
$A_i$=251,
$Z_i$=104
c) $^{122}$Sn($^{129}$Xe,pp), E/A=31MeV, $\theta_{av}$=25°
P= 660−750 MeV/c
$T_i$=10MeV
$T_i$=7MeV
$T_i$=5MeV
$A_i$=251,
$Z_i$=104
1 + R(q)
1.0
0.5
0
20
40
60
80
q [MeV/c]

Fig. 2

MSU-90-058

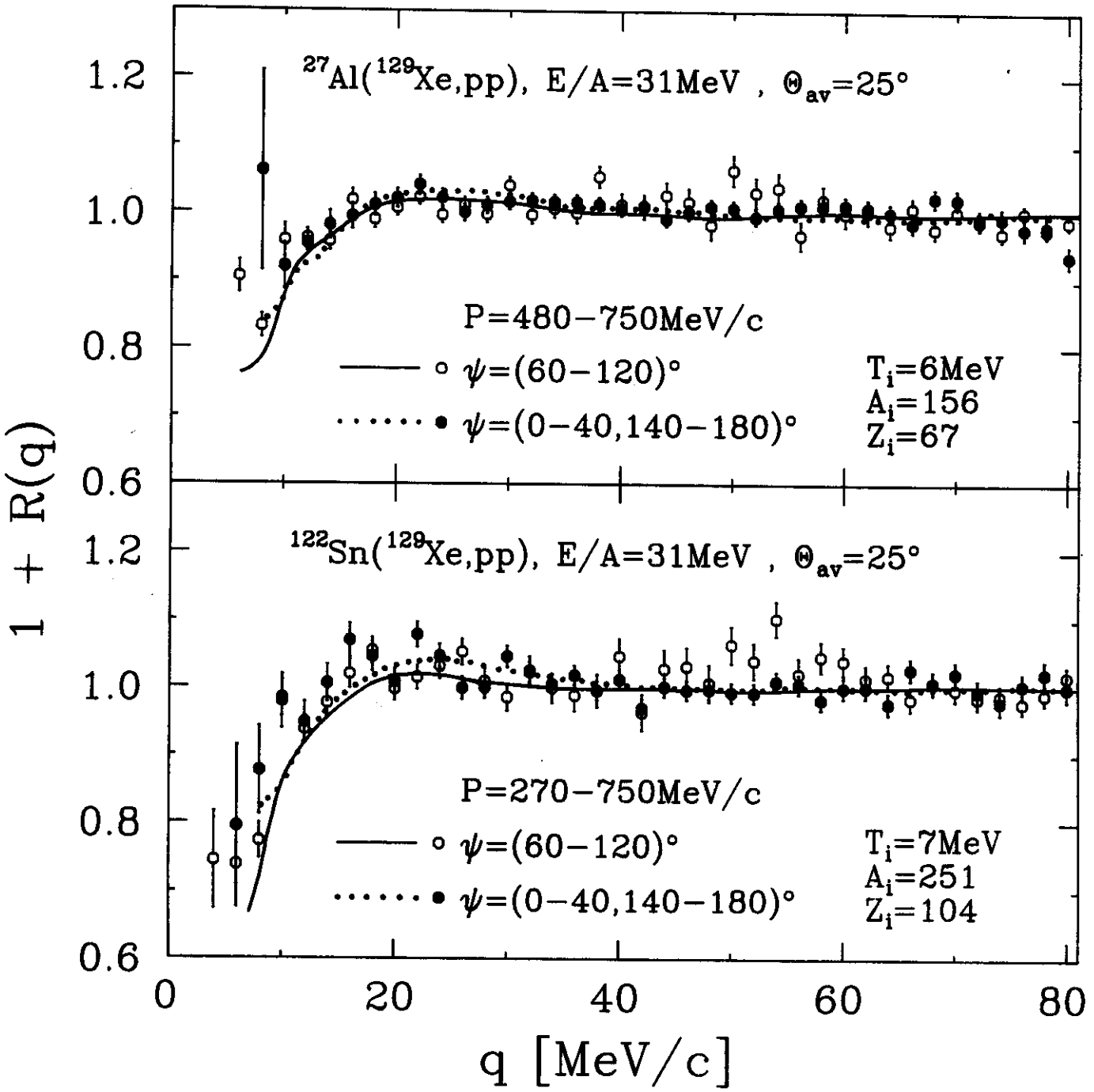


Fig. 3